Phytoliths as an indicator of change in vegetation related to the huge volcanic eruption at 7.3 ka in the southernmost part of Kyushu, southern Japan

Phytoliths as an indicator of change in vegetation related to the huge volcanic eruption at 7.3 ka in the southernmost part of Kyushu, southern Japan

Naoki Hayashi, Yudzuru Inoue, Tatsuichiro Kawano, Jun Inoue

Hayashi, N., Inoue, Y., Kawano, T., & Inoue, J. (2021). Phytoliths as an indicator of change in vegetation related to the huge volcanic eruption at 7.3 ka in the southernmost part of Kyushu, southern Japan. *The Holocene*. 31, 709–719. https://doi.org/10.1177/0959683620988057

Vegetation transition from the terminal Pleistocene to early Holocene reconstructed from phytolith records in the southernmost part of mainland Japan

Naoki Hayashi[a] & Jun Inoue[a]

[a] Department of Geosciences, Osaka Metropolitan University, 3-3-138 Sugimoto,

Sumiyoshi-ku, Osaka 558-8585, Japan

Corresponding author: Naoki Hayashi

E-mail: nhayashi5730@gmail.com

Highlights

- We examined phytolith records in the southernmost part of mainland Japan.

- Andropogoneae species flourished under forests in the late MIS 3.

- Grasslands covered in last glacial maximum (LGM).

- *Sasa* flourished on forest floor between ~18,000 and ~17,000 cal BP.

- Evergreen broad-leaved forests had developed at least until 7,300 cal BP.

Abstract

Phytolith records in paleosols provide valuable information on past vegetation *in situ*, especially for herbaceous plants. Although vegetation transition between the terminal Pleistocene and early Holocene in the southernmost parts of mainland Japan has been examined, detailed information on herbaceous plants during the period is scarce. Therefore, this study examined phytolith records in paleosols in the region to reconstruct the vegetation transition from the terminal Pleistocene to the early Holocene, focusing on herbaceous vegetation. Additionally, the combination of our phytolith and previous palynological records enable us to reconstruct vegetation transition in detail. Before ~30,000 cal BP, Andropogoneae species flourished under forest, comprising temperate pinaceous conifers, deciduous broad-leaved trees, and/or their adjacent area. In the Last Glacial Maximum (LGM), grasslands comprising Panicoideae, Chloridoideae, and Pooideae species were widely distributed under the influence of cool climate conditions and/or Aira caldera eruption. Furthermore, between ~18,000 and ~17,000 cal BP, *Sasa* flourished as a component of grassland or on forest floors, and then was gradually replaced by Andropogoneae species. Evergreen broad-leaved forests had developed at least by 7,300 cal BP in the study region.

1. Introduction

Glacial–interglacial climate dynamics have changed the vegetation distribution on earth. Notably, the last significant climatic changes from the last glacial period to the Holocene caused significant changes in composition and vegetation structures in most regions globally (Nolan et al., 2018). In modern Japan, each subarctic coniferous forest, cool-temperate deciduous broad-leaved forests, temperate coniferous forests, and warm-temperate evergreen broad-leaved forests have covered each region. Also, their distributions have varied significantly since the Last Glacial Maximum (LGM), reconstructed from records of pollen and plant fossils in sediment (e.g., Yasuda and Miyoshi, 1998; Ooi, 2016). However, these records lack detailed information on herbaceous vegetation.

In the southern Kyushu District, the southernmost part of mainland Japan, warm, temperate evergreen broad-leaved forests are locally distributed as natural forests in modern days. In contrast, in the LGM, temperate deciduous broad-leaved forests should have been distributed widely in this region, except for coastal areas where warm, temperate evergreen broad-leaved forests were possibly distributed (Nasu, 1980; Tsukada, 1985). However, few pollen records provide little information on the vegetation transition in this region. For example, in the late Marine Isotope Stage (MIS)

3, a mixed forest comprising temperate pinaceous conifers and temperate deciduous broad-leaved trees was distributed (Hase and Hatanaka, 1984; Iwauchi and Hase, 1995). Additionally, evergreen broad-leaved forests were distributed in the early Holocene (Matsushita, 2002). As mentioned above, the detailed vegetation types and their transition in the region are still poorly understood, especially for the grass component of herbaceous vegetation.

Phytolith records in paleosols provide valuable information on past vegetation *in situ*, especially herbaceous vegetation (e.g., Fredlund and Tieszen, 1997; Blinnikov et al., 2002; Miyabuchi and Sugiyama, 2019). Thus, this study examined phytolith assemblages in paleosols formed from late MIS 3 to early MIS 1 in the southernmost part of Kyushu District, reconstructing past vegetation and focusing on herbaceous vegetation. Further, we comprehensively reconstructed vegetation transition in the region by combining our phytolith records and palynological records in previous studies.

2. Study Region

The study region is the southern part of the Kyushu District, the southernmost part of the Japanese mainland. The Satsuma and Osumi Peninsula are situated in the region (Figure

1). The annual temperature (1991–2020) is 18.3°C and 16.4°C at Ibusuki Climatological Station (31°15'00" N, 130°38'12" E; elevation of 5 m) in the Satsuma Peninsula and Tashiro Climatological Station (31°11'54" N, 130°50'36" E; elevation of 182 m) in the Osumi Peninsula, respectively. The annual precipitation (1991–2020) is 2602.1 mm and 2888.2 mm at Ibusuki Climatological Station in the Satsuma Peninsula and Tashiro Climatological Station in the Osumi Peninsula, respectively (Japan Meteorological Agency, 2021). Therefore, the climate of both peninsulas is assigned to a warm temperate zone. Although plantation forests of *Cryptomeria japonica* and *Chamaecyparis obtusa* or secondary forests cover most regions, natural forests are distributed locally. The natural forest comprises warm temperate evergreen broad-leaf trees, except in mountain areas in the Osumi Peninsula; i.e., in the lowlands, the forest is mainly composed of *Symplocos glauca* and *Castanopsis sieboldii*, and above 400–500 m in altitude, the forest comprises *Distylium racemosum* and *Quercus salicina.* In addition, mixed forests composed of temperate deciduous broad-leaved trees and temperate pinaceous conifers, such as *Abies firma*, are distributed around the summit of the Kimotsuki Mountains in the Osumi Peninsula (Miyawaki, 1981).

3. Methods

3.1 Materials

We collected soil samples from outcrops using a plastic cube (2 × 2 × 2 cm) at three sites

for phytolith analysis. Site 1 (31°16'59"N, 130°34'26"E) is located at the Satsuma

Peninsula. Sites 2 (31°16'05"N, 130°52'01"E) and 3 (31°18'24"N, 130°52'46"E) are

located at the Osumi Peninsula (Figure 1). Figure 2 shows the geological columnar

sections at the respective sites, indicating lithofacies, soil colors, and sampling levels.

Either Osumi pumice fall (A-Os) or Aira-Tanzawa volcanic ash (AT) layer was found at

all sites, which erupted from Aira caldera (Figure 1) at 30,000 cal BP (Kobayashi et al.,

1983; Smith et al., 2013). Kikai-Akahoya volcanic ash (K-Ah), which erupted from the

Kikai caldera (Figure 1) at 7,300 cal BP (Machida and Arai, 1978; Smith et al., 2013),

was found at Site 3. Paleosols lie under and over the A-Os at Site 1, under the A-Os at

Site 2, and between the AT and the K-Ah at Site 3. Sakurajima-Satsuma volcanic ash (Sz-

S), which erupted from Mt. Sakurajima (Figure 1) at 12,800 cal BP (Okuno et al., 1997),

included in the middle part of the paleosols at Site 3.

We dated two paleosol layers at Site 3 using AMS radiocarbon measurement of

humin fractions extracted from soils by chemical treatment (Figure 2 and Table 1).

Additionally, we calibrated radiocarbon dates to calendar years using Calib Rev 8.1 and

the IntCal20 calibration dataset (Reimer et al., 2020). We constructed the age model of

paleosol layers at Site 3 based on the calibrated radiocarbon ages of humin and volcanic

ashes (Supplementary Figure 1).

3.2 Phytolith analysis

First, we collected a 1-cm^3 subsample from each soil sample. Furthermore, we extracted

phytoliths from the subsamples following the method proposed by Kawano et al. (2007)

and Okunaka et al. (2012). A known number of glass beads (approximately 200,000

grains) were added to each subsample to estimate the phytolith concentration (Fujiwara,

1976). Organic matter was oxidized with 30% H_2O_2 for 12 h at room temperature and 1

h at 250°C. Calcium carbonate was eliminated using 3 N HCl by heating in a water bath

for 1 h. Crays were removed by gravity sedimentation. The extracted phytoliths were

dried at 105°C for 24 h. We mounted a portion of the extraction residue on a glass slide

using a mounting medium (Eukitt). Then, we observed and counted the phytolith under a

transmission-type optical microscope at 400× magnification until we counted 300 glass

beads. Finally, we calculated phytolith concentration (grains•cm^{-3}) based on the observed

number of glass beads and phytoliths on the glass slide.

Phytoliths were identified according to the International Code for Phytolith

Nomenclature 2.0 (ICPN 2.0) (Neumann et al., 2019). Also, some phytolith types were classified into further sub-categories (Figure 4 and Table 2). For example, the BULLIFORM FLABELLATE phytoliths (ICPN 2.0) were further divided into four sub-types: *Sasa*-type, *Pleioblastus*-types, Bumbusoideae-types, Andropogoneae-types, following Sase and Kondo (1974), Sugiyama and Fujiwara (1986), Kondo and Sase (1986), Kawano et al. (2012), Inoue et al. (2016), and Hayashi et al. (2019; 2021). Most of the BLOCKY (ICPN 2.0) was identified as Panicoideae-type, following Sugiyama et al. (1988). Additionally, SADDLE was divided into Bambusoid-type and Chloridoid-type. Bambusoid-type corresponds to the collapsed saddle type in Piperno and Pearsall (1998).

The tree-type phytoliths, POLYHEDRAL FACETATE, ELONGATE GENICULATE SINUATE, and ELONGATE BRACHIATE ENTIRE were identified as *Castanopsis*-type, *Litsea*-type, *Distylium*-type, respectively, inferred from Kawano (2008). Furthermore, IRREGULAR SINUATE was identified as jigsaw puzzle-type produced from broad-leaved trees and ferns (*Pteridum*) in Japan (Kawano, 2008; Kondo, 2010).

4. Results

The phytolith analysis results are shown in Figure 4, Figure 5, and Supplementary Table 1. Diagrams were drawn using TILIA 2.1.1 (www.tiliait.com). The phytolith assemblages

were divided into five phytolith zones, A, B, C, D, and E, based on percentages of phytoliths.

Zone A is assigned to the phytolith assemblage in the paleosol layer under A-Os layers at Sites 1 and 2. This zone is dominated by Andropogoneae-type bulliform cells (Site 1: 27.1%–33.8%; Site 2: 12.4%–25.3%) and ELONGATE (Site 1: 17.2%–22.7%; Site 2: 18.9%–26.7%) phytoliths. Additionally, a percentage of *Sasa*-type bulliform cell phytolith is observed (Site 1: 9.0%–13.8%; Site 2: 3.1%–10.1%). Bambusoideae-type bulliform cell phytolith accounts for 1.8%–4.8% at Site 1 and 1.4%–5.7% at Site 2. In short cells, the Bambusoid-type is common (Site 1: 5.7%–13.3%; Site 2: 4.3%–26.8%). Few BILOBATE and Chloridoid-type phytoliths occur (BILOBATE: <4.8%; Chloridoid-type: <3.5%); other short cell types are rare (<1.4%). ACUTE BULBOSUS phytolith occurs in small amounts (Site 1: 1.5%–2.5%; Site 2: 1.3%–4.3%), and jigsaw puzzle-type phytoliths occur in some layers (<1%). The phytolith concentrations in this zone are 2.1×10^5–4.2×10^5 grains·cm^{-3} at Site 1 and 1.1×10^5–40.2×10^5 grains·cm^{-3} at Site 2, respectively. Moreover, the concentration is very high (18.8×10^5–40.2×10^5 grains·cm^{-3}) under A-Os layer at Site 2.

Zone B is assigned to the phytolith assemblage in the lower part of paleosol layers between K-Ah and A-Os or AT layers at Sites 1 and 3. The abundance of short cells

characterizes this zone. BILOBATE (Site 1: 7.4%–14.1%; Site 3: 10.8%–20.6%) and

RONDEL (Site 1: 4.1%–8.4%; Site 3: 5.6%–11.1%) phytoliths have the highest

percentages in all zones. Bambusoid-type (Site 1: 9.2%–17.4%; Site 3: 6.9%–18.3%) and

Chloridoid-type (Site 1: 5.6%–15.1%; Site 3: 0.0%–3.4%) phytoliths are common. A

percentage of CRENATE phytoliths is observed at Site 1 (1.6%–3.0%). However, in

bulliform cells, *Sasa*-type phytoliths account for 4.6%–10.7% at Site 1 and 1.8%–10.1%

at Site 3. Andropogoneae-type phytoliths are low relative to Zone A (Site 1: 6.3%–11.2%;

Site 3: 5.5%–8.9%). However, ELONGATE and ACUTE BULBOSUS phytoliths account for

13.0%–26.4% and 1.7%–3.8%, respectively, and no tree phytoliths is observed in this

zone. The phytolith concentrations are 0.7×10^5–3.1×10^5 grains·cm^{-3} at Site 1 and 1.2

$\times 10^5$–1.4×10^5 grains·cm^{-3} at Site 3, respectively.

Zone C is assigned to phytolith assemblages in the lower middle part of the

paleosol layers between K-Ah and A-Os or AT layers at Sites 1 and 3. This zone is

characterized by the dominance of *Sasa*-type bulliform cell phytoliths (Site 1: 12.6%–

24.4%; Site 3: 26.7%–34.6%). At Site 1, *Sasa*-type phytoliths show an upward increase.

Andropogoneae-type bulliform cell phytoliths are common (Site 1: 4.9%–10.1%; Site 3:

4.8%–10.3%). In short cells, Bambusoid-type phytoliths are abundant (Site 1: 15.0%–

29.6%; Site 3: 12.2%–28.0%). At Site 1, Chloridoid-type, BILOBATE, and RONDEL short

cell phytoliths show an upward decrease in this zone (Chloridoid-type: 3.9%–8.9%, BILOBATE: 3.4%–8.3%, and RONDEL: 1.5%–4.3%). At Site 3, short cell phytoliths, except for Bambusoid-type, are rare (0.0%–3.7%). ELONGATE and ACUTE BULBOSUS phytoliths account for 11.7%–19.3% at Site 1 and 8.4%–15.3% at Site 3, and 0.8%–2.5% at Site 1 and 2.2%–4.0% at Site 3, respectively. Jigsaw puzzle-type phytoliths occur in some layers (<1%). The phytolith concentrations show a gradual upward increase at both sites (2.5×10^5–7.0×10^5 grains·cm^{-3} at Site 1 and 1.7×10^5–13.2×10^5 grains·cm^{-3} at Site 3).

Zone D is assigned to the phytolith assemblages in the upper middle part of paleosol layers between K-Ah and A-Os or the AT layers at Site 3. This zone is characterized by the abundance of Bambusoid-type short cell phytoliths (13.9%–34.3%). The percentage of *Sasa*-type bulliform cell phytoliths was lower than zone C (8.7%–20.0%). Also, a percentage of Andropogoneae-type bulliform cell (5.0%–15.7%), BILOBATE (1.8%–10.0%), and RONDEL (1.2%–11.2%) short cell phytoliths were observed. Few Bambusoideae-type bulliform cells (1.2%–4.7%), Chloridoid-type (0.7%–5.2%), and ACUTE BULBOSUS (0.9%–5.2%) phytoliths occurred, and ELONGATE phytoliths accounted for 8.0%–16.8%. The phytolith concentration is 1.8×10^5–16.6×10^5 grains·cm^{-3}.

Zone E is the phytolith assemblage in the uppermost part of paleosol layers

between K-Ah and A-Os or the AT layers at Site 3. This zone is characterized by phytoliths derived from evergreen broad-leaved tree species. *Castanopsis-* and *Distylium-* type phytoliths are observed in some layers (<1%), and *Litsea*-type phytoliths occur at the upper part of this zone (<1.6%). In bulliform cells, Andropogoneae-type phytoliths are abundant (11.2%–27.5%). A certain percentage of *Sasa*-type bulliform cells (4.3%–13.2%) and Bambusoid-type short cells (5.6%–14.7%) phytoliths were observed. Few Bambusoideae-type bulliform cells (1.6%–4.9%), Chloridoid-type (1.3%–4.2%), BILOBATE (1.4%–8.6%), RONDEL (0.3%–4.4%), and ACUTE BULBOSUS (1.1%–3.3%) phytoliths occurred. ELONGATE phytoliths accounted for 9.9%–16.2%. The phytolith concentration is 1.1×10^5–4.4×10^5 grains·cm^{-3}.

5. Discussion

5.1 Vegetation history around the study sites reconstructed from phytolith records

Table 2 summarizes plant families and genera that produce phytolith types identified in this study and their habitat and climate zones. *Sasa*, *Miscanthus-Sasa*, and *Miscanthus-Pleioblastus* grasslands are distributed in subarctic, cool-temperate, and warm-temperate zones, respectively (Numata, 1969; 1974). Consequently, *Sasa*, *Pleioblastus*, and *Miscanthus* are distributed in subarctic to cool-temperate, warm-temperate, and cool-

temperate to warm-temperate zones, respectively, as a component of grassland. *Sasa* is also a significant component of deciduous broad-leaved forest understories in cool-temperate zone (Shidei, 1974). Although Chloridoideae and Pooideae are hardly dominant in grassland without grazing pressure in Japan, Chloridoideae is prone to grow in bare land in the temperate zone. In Japan, deciduous broad-leaved forests are distributed in the cool-temperate zone, whereas evergreen forests are distributed in the warm-temperate zone (Numata, 1969). *Castanopsis*, *Distylium*, and *Litsea* are components of the warm-temperate and subtropical evergreen forest. *Pteridium*, a fern, is a component of grassland in cool-temperate to subtropical zone. Therefore, we reconstructed vegetation transitions, and past climate conditions in the region from the phytolith records obtained at the study sites, based on their attributing plants and inhabit the conditions shown in Table 2.

Phytolith assemblages in Zone A are characterized by the dominance of Andropogoneae-type bulliform cell and Bambusoid-type short cell phytoliths with Sasa-type bulliform cell phytolith, and jigsaw puzzle-type phytoliths (Figure 4). Andropogoneae-type bulliform cell phytoliths are produced from Andropogoneae (Kondo and Sase, 1986; Sugiyama and Fujiwara, 1986; Kawano et al., 2012), and the Bambusoideae genera are prone to produce Bambusoid-type short cell phytoliths (Kondo

and Ohtaki, 1992; Kondo, 2010). Thus, the dominance of these genera implies that Andropogoneae species flourished with some Bambusoideae species such as *Sasa*. Additionally, the high phytolith concentrations in this zone may imply that the adjacent area of Site 2 was covered densely by the genus. Furthermore, the occurrence of jigsaw puzzle-type phytoliths suggests that broad-leaved tree species or ferns were distributed because jigsaw puzzle-type phytoliths are produced by broad-leaved trees and *Pteridium* species in Japan. (Kawano, 2008; Kondo, 2010).

The phytolith records in Zone B are characterized by the high percentage occurrence in short cell phytoliths, especially BILOBATE and RONDEL (Figures 4 and 5). BILOBATE short cell phytoliths are generally produced from Panicoideae, Chloridoideae, and Arundinoideae, and RONDEL short cell phytoliths are derived from Pooideae and Chloridoideae (ICPN2.0, Neumann et al., 2019). Since Arundinoideae species are prone to produce bulliform cell phytoliths (Chen et al., 2020), the low percentage occurrence in bulliform cell phytoliths implies that no or few Arundinoideae species stood. The percentage of Andropogoneae-type bulliform cell phytoliths in this zone is lower than those in Zone A, suggesting that Andropogoneae genera belonging to Panicoideae decreased after ~30,000 cal BP. Thus, we assume that the grasslands of Panicoideae, Chloridoideae, and Bambusoideae species were distributed.

The phytolith assemblage in Zone C is characterized by a high percentage of *Sasa*-type bulliform cells and Bambusoid-type short cell phytoliths and a low percentage of other SADDLE, BILOBATE, and RONDEL short cell phytoliths relative to other zones (Figure 5). *Sasa*-type bulliform cell phytoliths are produced from *Sasa* (Sugiyama and Fujiwara, 1986; Kawano et al., 2012). The phytolith assemblage and the increasing trend of phytolith concentrations indicate that *Sasa* replaced Panicoideae and Chloridoideae species at the beginning of the zone and flourished afterward. *Sasa* grows as a component of grassland and deciduous broad-leaved forest understory (Shidei, 1974). Additionally, jigsaw puzzle-type phytoliths produced from broad-leaved trees and/or ferns occur in this zone (Figure 5). Therefore, the area was presumably covered by *Sasa* grassland with ferns or deciduous broad-leaved trees with *Sasa* flourishing on their floor.

In Zone D, the percentage of Andropogoneae-type bulliform cell and BILOBATE short cell phytoliths increased gradually upward, and the percentage of *Sasa*-type gradually decreased upward (Figure 5). These suggest that Andropogoneae species had gradually replaced *Sasa* species in this zone.

Phytolith assemblages in Zone E are characterized by the appearance and increasing upward of evergreen broad-leaved species phytoliths (*Castanopsis*-, *Litsea*-, and *Distylium*-types) (Figure 5). From modern observations of phytolith assemblages, even

in Japanese forest soils, phytoliths derived from arboreal species are less than one-fifth of that of Poaceae-derived phytoliths (Kondo and Sase, 1990). Nevertheless, a certain percentage occurrence and increase in the phytoliths indicate that the evergreen broad-leaved forest had developed in this zone. Furthermore, the higher percentage of Andropogoneae-type bulliform cell phytoliths implies that Andropogoneae species flourished at that time.

Zone A laid under A-Os or AT tephra presumably corresponds to before ~30,000 cal BP based on the date of the Aira caldera eruption. Zone B lies between the A-Os and the soil layers dated at 18,000–19,000 cal BP at Site 3. Thus, the phytolith assemblages potentially represent the vegetation during a certain time between ~30,000 cal BP and ~18,000 cal BP. Although the exact period of Zone B is unclear, it is assumed that the zone includes phytolith assemblages at a period during the LGM of 24–18 ka (Mix et al., 2001). Zone C lies between the soil layers dated at ~18,000 cal BP and ~17,000 cal BP, respectively, suggesting that the phytolith assemblage in this zone represents vegetation during this period. Additionally, Zones D and E lie between Sz-S and K-Ah, indicating phytolith assemblage representing vegetation between ~12,800 cal BP and ~7,300 cal BP corresponding to early Holocene.

Thus, the vegetation change in the study region reconstructed from our phytolith

records is summarized as follows. Before ~30,000 cal BP, Andropogoneae species and

Sasa were dominant. In the LGM, the grasslands of Panicoideae, Chloridoideae, and

Bambuoideae developed. Also, between ~18,000 cal BP and ~17,000 cal BP, *Sasa*

flourished as grassland with ferns or deciduous broad-leaved forests floor vegetation.

From the terminal Pleistocene (~17,000 cal BP) to the early Holocene, *Sasa* had been

gradually replaced by Andropogoneae species. Then, evergreen broad-leaved forests

composed of *Litsea* and *Distylium*, and other species had developed until 7,300 cal BP.

5.2 Vegetation transition reconstructed from phytolith and pollen records

We compared phytolith records in this study to pollen records in the study region between

terminal Pleistocene and early Holocene (Figure 6). Then, we reconstructed the

vegetation from these records and assessed the relationship between vegetation transition

and global climate change or regional context.

      We presume that at ~30,000 cal BP corresponding to late MIS 3, Andropogoneae

species were dominant based on the phytolith records. Also, pollen records reported in

previous studies show that mixed forests are mainly composed of temperate pinaceous

conifers, such as *Pinus*, *Abies*, *Tsuga*, and temperate deciduous broad-leaved trees,

Carpinus and *Quercus* subgen. *Lepidobalanus* developed (Hase and Hatanaka, 1984;

Iwauchi and Hase, 1995). Furthermore, wood fossils of Fagaceae and *Pinus* subgen.

Diploxylon were found in loam under the AT layer in the Satsuma Peninsula (Paleoenvironment Research Co., Ltd, 2013). Considering these findings, mixed forests mainly comprising temperate pinaceous conifers and temperate deciduous broad-leaved trees are developed, and Andropogoneae species likely flourished in the forest and/or its adjacent areas in the late MIS 3. Furthermore, the mixed forest developed at that time indicates that the study region belonged to the intermediate between cool- and warm-temperate zones, based on their distribution in modern Japan (Nozaki, 2005). This is consistent with the dominance of Andropogoneae species, distributed widely in cool-temperate to warm-temperate zones.

Pollen records during the LGM in eastern Asia suggest that deciduous broad-leaved forests likely developed in southern China inlands and Kyushu District Japan (Kawahata and Ohshima, 2004; Yue et al., 2012). However, our phytolith records suggest that the grasslands of Panicoideae, Chloridoideae, and Bambusoideae developed around the study region without forest development in the LGM (Figure 6). The grassland may be partially attributed to the cool and dry conditions in the LGM. In addition to the climatic condition, Nasu (1980) assumed that grassland development in this region was due to the influence of the tephra that erupted from Aira caldera at 30,000 cal BP. Specifically, tephra

deposition devastated the original forests and prevented their regeneration. Additionally, Panicoideae and Chloridoideae species grew on barren land, resulting in the grassland maintenance for a long time. Thus, the eruption and/or the climate conditions presumably contributed to the grassland development during this period. Furthermore, the pollen data imply that some evergreen forests stood in the southernmost part of Kyusyu Island in the LGM (Matsuoka, 1994), similar to southeastern China and Ryukyu Islands (Dai et al., 2021; Kuroda and Ozawa, 1996). However, previous (Sugiyama, 1999; 2002) and present phytolith studies show that evergreen broad-leaved trees were never distributed at any sites in the study region. Therefore, the evergreen broad-leaved trees' distribution was presumably limited to the coastal areas at that time (Figure 1) under the influence of a warm ocean current.

Our phytolith records indicate that *Sasa* replaced Panicoideae and Chloridoideae species and flourished between ~19,000 and ~18,000 cal BP. *Sasa* development might be due to fertile soil formation after the long time elapsed after the Aira caldera eruption. This is because *Sasa* is hardly prone to grow on the sand ground (Shibata, 2015) like volcanic ejecta. The developing *Sasa* communities presumably had prevented Panicoideae and Chloridoideae species from growing because dwarf bamboo, such as *Sasa*, suppresses other species and reduced species diversity (Kudo et al., 2017). The

absence of evergreen broad-leaved tree phytoliths indicates that evergreen broad-leaved trees were never distributed in the area, although the vegetation type is poorly understood.

Our phytolith records show that *Sasa* had been gradually replaced by Andropogoneae species since 17,000 cal BP. Although we have no pollen record in late MIS 2, those in early MIS 1 indicate that temperate deciduous broad-leaved forests of *Carpinus*, *Quercus* subgen. *Lepidobalanus,* and *Ulmus-Zelkova* were distributed in the southernmost part of the Kyushu District (Iwauchi and Hase, 1996; Matsushita, 2002). Thus, the temperate deciduous broad-leaved trees were presumably distributed with Andropogoneae and Bambusoideae species between the terminal Pleistocene and early Holocene. The proportions of the herbaceous plants changed temporally, and the proportion change is possibly related to the climatic warming from MIS 2 to MIS 1.

The presence of evergreen broad-leaved species phytoliths indicates that evergreen broad-leaved trees stood in the early Holocene. Evergreen broad-leaved species phytoliths in paleosol under the K-Ah layer have also been found at other sites in the study region (Hayashi et al., 2021; Sugiyama 1999; 2002). Furthermore, pollen records show that *Castanopsis* and *Q.* subgen. *Cyclobalanopsis* pollens are extremely dominant in the early Holocene sediments (Iwauchi and Hase, 1996; Matsushita, 2002). These findings suggest that evergreen broad-leaved forests were distributed widely in the southernmost part of

the Kyushu District in the early Holocene. The expansion of the forests presumably resulted from the climatic warming at that time.

6. Conclusion

We reconstructed the vegetation transition from late MIS 3 to early MIS 1 by combining phytolith records in this study and palynological records in previous studies in the southernmost part of Kyushu District, southern Japan. Before ~30,000 cal BP, mixed forests composed of temperate pinaceous trees and temperate deciduous broad-leaved trees, and Andropogoneae species flourished in the forest and/or adjacent areas under warm climate conditions in the late MIS 3. In the LGM, grasslands composed of Panicoideae, Chloridoideae, and Pooideae species mostly covered the study region under the influence of cool climate conditions and/or Aira caldera eruption. In the terminal Pleistocene, *Sasa* flourished as a component of grassland or deciduous broad-leaved forest understory between ~18,000 and ~17,000 cal BP, and no evergreen broad-leaved trees likely stood. Since ~17,000 cal BP, *Sasa* had been gradually replaced by Andropogoneae species. Then, evergreen broad-leaved forests were developed and distributed widely in the southernmost part of the Kyushu District, at least by 7,300 cal BP.

Reference

Blinnikov, M., Busacca, A., Whitlock, C., 2002. Reconstruction of the late Pleistocene grassland of the Columbia basin, Washington, USA, based on phytolith records in loess. Palaeogeography, Palaeoclimatology, Palaeoecology 177, 77–101. https://doi.org/10.1016/S0031-0182(01)00353-4

Chen, I., Li, K., Tsang, C., 2020. Silicified bulliform cells of Poaceae: morphological characteristics that distinguish subfamilies. Botanical studies 61, 5 https://doi.org/10.1186/s40529-020-0282-x

Dai, L., Li, S., Yu, J., Wang, J., Peng, B., Wu, B., Lao, J., Zhang, Q., Hao, Q., 2021. Palynological evidence indicates the paleoclimate evolution in southeast China since

late marine isotope stage 5. Quaternary Science Reviews 266, 106964. 10.1016/j.quascirev.2021.106964

Fredlund, G. G., Tieszen, L. L., 1997. Phytolith and Carbon Isotope Evidence for Late Quaternary Vegetation and Climate Change in the Southern Black Hills, South Dakota. Quaternary Research 47, 206–217. https://doi.org/10.1006/qres.1996.1862

Fujiwara, H., 1976. Fundamental studies of plant opal analysis: on the silica bodies of motor cell of rice plants and their near relatives, and the method of quantitative analysis. Archaeology and Natural Science (Biannual Journal of the Japanese Societies on Cultural Property) 9 15–29. (in Japanese)

Hase, Y., Hatanaka, K., 1984. Pollen stratigraphical study of the Late Cenozoic sediments in Southern Kyushu, Japan. The Quaternary Research (*Daiyonki-Kenkyu*) 23, 1–20. (in Japanese) https://doi.org/10.4116/jaqua.23.1

Hayashi, N., Kawano, T., Inoue, J., 2019. Long-term response of respective grass types to variations in fire frequency in central Japan, inferred from phytolith and macrocharcoal records in cumulative soils deposited during the Holocene. Quaternary International 527, 94–102. https://doi.org/10.1016/j.quaint.2018.04.048

Hayashi, N., Inoue, Y., Kawano, T., Inoue, J., 2021. Phytoliths as an indicator of change in vegetation related to the huge volcanic eruption at 7.3 ka in the southernmost part of

Kyushu, southern Japan. The Holocene 31, 709–719.

https://doi.org/10.1177/0959683620988057

Inoue, J., Okunaka, R., Kawano, T., 2016. The relationship between past vegetation type

and fire frequency in western Japan inferred from phytolith and charcoal records in

cumulative soils. Quaternary International 397, 513–522.

https://doi.org/10.1016/j.quaint.2015.02.039

Iwauchi, A., Hase, Y., 1995. Pollen analysis of the Mizozono Formation (Late

Pleistocene) in the Kakuto Basin, Southern Kyushu, Japan Memoirs of the Faculty of

General Education, Kumamoto University Natural sciences 30, 155–169. (in Japanese)

Iwauchi, A., Hase, Y., 1996. Pollen analyses of Holocene sediments of Beppu Bay and

alluvium of Kagoshima Plain. Memoirs of the Faculty of General Education,

Kumamoto University Natural sciences 31, 119–130. (in Japanese)

Japan Metrological Agency, 2021. Normal Value of Automated Meteorological Data

Acquisition System (1991–2020). Available at Japan Metrological Agency web site:

https://www.data.jma.go.jp/gmd/risk/obsdl/index.php.

Kawahata, H., Ohshima, H., 2004. Vegetation and environmental record in the northern

East China Sea during the late Pleistocene Global and Planetary Change 41, 251–273.

https://doi.org/10.1016/j.gloplacha.2004.01.011

Kawano, T., 2008. Morphology of leaf phytoliths in selected tree species of Japan. Bulletin of the Kyoto Prefectural University Forests 49, 19–31. (in Japanese)

Kawano, T, Takahara, H, Nomura, T, Shibata, H, Uemura, S, Sasaki, N, Yoshioka, T, 2007. Holocene phytolith record at Picea glehnii stands on the Dorokawa Mire in northern Hokkaido, Japan. The Quaternary Research (*Daiyonki-Kenkyu*) 46, 413–426. https://doi.org/10.4116/jaqua.46.413

Kawano, T., Sasaki, N., Hayashi, T., Takahara, H., 2012. Grassland and fire history since the late-glacial in northern part of Aso Caldera, central Kyusyu, Japan, inferred from phytolith and charcoal records. Quaternary International 254, 18–27. https://doi.org/10.1016/j.quaint.2010.12.008

Kobayashi, T., Hayakawa, Y., Aramaki, S, 1983. Thickness and Grain-size Distribution of the Osumi Pumice Fall Deposit from the Aira Caldera. Bull.Volcanol. Sac. Japan, Ser.2 28, 129–139. https://doi.org/10.18940/kazanc.28.2_129

Kondo, R., 2010. Phytolith atlas. 387pp. Hokkaido University Press, Sapporo. (in Japanese).

Kondo, R., Ohtaki, M., 1992. Opal phytoliths originated from the short cell in leaves of Bambusoideae. Reports of the Fuji Bamboo Garden 36, 23–43 (in Japanese).

Kondo, R., Sase, T., 1986. Opal phytolith, their nature and application. The Quaternary

Research (*Daiyonki-Kenkyu*) 25, 31–63. (in Japanese)

https://doi.org/10.4116/jaqua.25.31

Kondo, R., Sase, T., 1990. Opal phytolith analysis of Japanese soil with regard to interpretation of paleovegetation. 14th international congress of soil science transaction, commission V, Kyoto, Japan pp.372–373.

Kudo, G., Kawai, Y., Amagai, Y., Winkler D.E., 2017. Degradation and recovery of an alpine plant community: experimental removal of an encroaching dwarf bamboo. Alpine Botany 127, 75–83. https://doi.org/10.1007/s00035-016-0178-2

Kuroda, T., Ozawa, T., 1996. Paleoclimatic and Vegetational Changes during the Pleistocene and Holocene in the Ryukyu Islands inferred from Pollen Assemblages. Journal of Geography 105, 328–342. (in Japanese)

https://doi.org/10.5026/jgeography.105.3_328

Lisiecki, L. E., Raymo, M. E., 2005. A Pliocene-Pleistocene stack of 57 globally distributed benthic delta O-18 records. Paleoceanography 20, PA1003.

Machida, H., Arai, F., 1978. Akahoya Ash—A Holocene Widespread Tephra Erupted from the Kikai Caldera, South Kyushu, Japan. The Quaternary Research (*Daiyonki-Kenkyu*) 17, 143–163. (in Japanese) https://doi.org/10.4116/jaqua.17.143

Matsuoka, K., 1994. Geographical Distribution of the Japanese Laureal Forests at the Last

Glacial Age —Pollen Assemblage of ca. 24,000yBP. in a Core Sample Collected from

the Danjo Basin in the East China Sea—. Japanese Journal of Palynology 40 13–24.

(in Japanese)

Matsushita, M., 2002. Vegetation Changes under the Influence of the Kikai-Akahoya

Eruption in Osumi Peninsula, Southern Kyushu, Japan. The Quaternary Research

(*Daiyonki-Kenkyu*) 41, 301–310. (in Japanese) https://doi.org/10.4116/jaqua.41.301

Mix. A., Bard, E., Schneider, R., 2001. Environmental processes of the ice age: land,

oceans, glaciers (EPILOG). Quaternary Science Reviews 20, 627–657.

https://doi.org/10.1016/S0277-3791(00)00145-1

Miyabuchi, Y., Sugiyama, S., 2019. Vegetation history after the late period of the Last

Glacial Age based on phytolith records in Nangodani Valley basin, southern part of the

Aso caldera, Japan. Journal of Quaternary Science 35, 304–315.

https://doi.org/10.1002/jqs.3153

Miyawaki, A., 1981. Vegetation of Japan Kyushu. 484pp. Shibundo, Tokyo. (in Japanese)

Nasu, T. 1980. On the vegetation of the Würm glacial maximum. "Biogeography since

the Würm glacial (Grantsin-Aid for Scientific Research Reports of Fiscal Year 1979),"

55–61. (in Japanese)

Neumann, K., Strömberg, C. A. E., Ball, T., Albert, R. M., Vrydagh, L., Cummings, L. S.,

2019. International Code for Phytolith Nomenclature (ICPN) 2.0. Annals of Botany 124 189–199. https://doi: 10.1093/aob/mcz064

Nolan, C., Overpeck, J. T., Allen, J. R. M. Anderson, P. M., Betancourt, J. L., Binney, H. A., Brewer, S., Bush, M. B., Chase, B. M., Cheddadi, R., Djamali, M., Dodson, J., Edwards, M. E., Gosling, W. D., Haberle, S., Hotchkiss, S. C., Huntley, B., Ivory, S. J., A. Kershaw, P., Kim, S. H., Latorre, C., Leydet, M., Lézine, A. M., Liu, K. B., Liu, Y., Lozhkin, A. V., McGlone, M. S., Marchant, R. A., Momohara, A., Moreno, P. I., Müller, S., Otto-Bliesner, B. L., Shen, C., Stevenson, J., Takahara, H., Tarasov, P. E, Tipton, J., Vincens, A., Weng, C., Xu, Q., Zheng, Z., Jackson, S. T., 2018. Past and future global transformation of terrestrial ecosystems under climate change. Science 923, 920–923. https://doi.org/10.1126/scien ce.aan5360

Nozaki, R., 2005. Vegetation in intermediate-temperate climate zone. Fukushima, T., Iwase, T. (Eds.) Illustrated Vegetation of Japan. Asakura Shoten, Tokyo, 62–67. (in Japanese)

Numata, M., 1969. Progressive and retrogressive gradient of grassland vegetation measured by degree of succession-Ecological judgement of grassland condition and trend IV. Vegetatio 19, 96–127.

Numata, M., 1974. Grassland Vegetation. Numata, M. (Eds), The flora and vegetation of

Japan. Kodansha, Tokyo and Elsevier Scientific Pub. Co., Amsterdam. 125–150.

Okunaka, R., Kawano, T., Inoue, J., 2012. Holocene history of intentional fires and grassland development on the Soni Plateau, Central Japan, reconstructed from phytolith and macroscopic charcoal records within cumulative soils, combined with paleoenvironmental data from mire sediments. The Holocene 22, 793–800. https://doi.org/10.1177/0959683611430409

Okuno, M., Nakamura, T., Moriwaki, H., 1997. AMS radiocarbon dating of the Sakurajima tephra group, Southern Kyushu, Japan. Nuclear Instruments and Methods in Physics Research Section B: Beam Interactions with Materials and Atoms 123 470–474. https://doi.org/10.1016/S0168-583X(96)00614-3

Ooi, N., 2016. Vegetation history of Japan since the last glacial based on palynological data. Japanese Journal of historical botany 25, 1–101. https://doi.org/10.34596/hisbot.25.1-2_1

Paleoenvironment Research Co., Ltd, 2013. Identification of wood fossil at Nishitaragasako archeological site. The Ibusuki Board of Education (Eds), Report of the Mizusako archaeological site vol. IV and Report of the Nishitaragasako archaeological site. The Ibusuki Board of Education, Kagoshima, 494–498. (in Japanese)

Piperno, D. R., Pearsall, R., 1998. The Silica Bodies of Tropical American Grasses: Morphology, Taxonomy, and Implications for Grass Systematics and Fossil Phytolith Identification. Smithsonian Contributions to Botany 85, 1–40. https://doi.org/10.5479/si.0081024X.85

Reimer, P. J., Austin, W. E. N., Bard, E., Bayliss, A., Blackwell, P. G., Ramsey, C. B., Butzin, M., Cheng, H., Edwards, R, L., Friedrich, M., Grootes, P, M., Guilderson, T. P., Hajdas, I., Heaton, T. J., Hogg, A. G., Hughen, K. A., Kromer, B., Manning, S, W., Muscheler, R., Palmer, J. G., Pearson, C van der Plicht, J., Reimer, R. W., Richards, D. A., Scott, E. M., Southon, J. R., Turney, C. S. M., Wacker, L., Adolphi, F., Büntgen, U Capano, M., Fahrni, S. M., Fogtmann-Schulz, A., Friedrich, R., Köhler, P., Kudsk, S., Miyake, F., Olsen, J., Reinig, F., Sakamoto, M., Sookdeo, A., Talamo, S., 2020. The IntCal20 Northern Hemisphere Radiocarbon Age Calibration Curve (0–55 cal kBP). Radiocarbon, 62, 725–757. https://doi.org/10.1017/RDC.2020.41

Tsukada, M., 1985. Map of vegetation during the Last Glacial Maximum in Japan. Quaternary Research 23, 369–381. https://doi.org/10.1016/0033-5894(85)90041-9

Sase, T., Kondo, R., 1974. The Study of Opal Phytoliths in the Humus Horizon of Buried Volcanic Ash Soils in Hokkaido, Series I. Research bulletin of Obihiro Zootechnical University 465–483. (in Japanese)

Shibata, S., 2015. Dwarf bamboo for a greening plant. Weeds and Vegetation Management 7, 20–29. (in Japanese)

Shidei, T., 1974. Forest Vegetation Zones. Numata, M (Eds), The flora and vegetation of Japan. Kodansha, Tokyo and Elsevier Scientific Pub. Co., Amsterdam, 87–124.

Smith, V. C., Staff, R. A., Blockley, S. P. E., Ramsey, R. B., Nakagawa, T., Mark, D. F., Takemura, K., Danhara, T., Suigetsu 2006 Project Members, 2013. Identification and correlation of visible tephras in the Lake Suigetsu SG06 sedimentary archive, Japan: chronostratigraphic markers for synchronizing of east Asian/west Pacific palaeoclimatic records across the last 150 ka. Quaternary Science Reviews 67, 121–137. http://dx.doi.org/10.1016/j.quascirev.2013.01.026

Sugiyama, S., 1999. Lucidophyllous Forest Development since the Last Glacial Age in Southern Kyushu, Japan, Clarified by Phytolith Studies. The Quaternary Research (*Daiyonki-Kenkyu*) 38, 109–123. (in Japanese) https://doi.org/10.4116/jaqua.38.109

Sugiyama, S., 2002. The Impact of the Kikai-Akahoya Explosive Eruption on Vegetation in Southern Kyushu, Japan, Clarified by Phytolith Studies. The Quaternary Research (*Daiyonki-Kenkyu*) 41, 311–316. (in Japanese) https://doi.org/10.4116/jaqua.41.311

Sugiyama, S., Fujiwara, H., 1986. The shape of silica bodies in the motor cells of

Bambusoideae. Archaeology and Natural Science 19, 69–84. (in Japanese)

Sugiyama, S., Matsuda, R., Fujiwara, H., 1988. Morphology of phytoliths in the motor cells of Paniceae Basic study on the ancient cultivation. Archaeology and Natural Science (Biannual Journal of the Japanese Societies on Cultural Property) 20, 81–92 (in Japanese).

Tsukada, M., 1985. Map of vegetation during the Last Glacial Maximum in Japan. Quaternary Research, 23, 369–381. https://doi.org/10.1016/0033-5894(85)90041-9

Twiss, P.C., Suess, E., Smith, R.M., 1969. Morphological classification of grass phytoliths. Soil Science of America, Proceedings 33, 109–115.

Yasuda, Y., Miyashi, N., 1998. Illustrated Vegetation History of Japanese Archipelago. 302pp. Asakurashoten, Tokyo. (in Japanese)

Yue, Y., Zheng, Z., Huang, K., Chevalier, M., Chase, B., Carré, M., Ledru, M., Cheddadi, R., 2012. A continuous record of vegetation and climate change over the past 50,000 years in the Fujian Province of eastern subtropical China. Palaeogeography, Palaeoclimatology, Palaeoecology 365–366, 115–123.

Figure captions

Figure 1. Maps of (A) mainlands Japan showing Kyushu District, (B) the southern

Kyushu District showing the location of the volcano related to this study and the

previous palynological study sites, and (C) the southernmost part of the Kyushu

District showing the sampling sites in this study. The pollen records at site 1, 2, 3,

and 4 were reported by Hase and Hatanaka (1984), Iwauchi and Hase (1995),

Iwauchi and Hase (1996), Matsushita (2002), respectively. The dotted line in map

of the southern Kyushu District (B) indicates the assumed coastline of the Last

Glacial Maximum (~20,000 years ago). The base map is the digital map released

by the Geospatial Information Authority of Japan (maps.gsi.go.jp/).

Figure 2. Geological columnar sections at the study sites indicating lithofacies, grain size,

and sampling level. Abbreviations for the tephra names and their eruption ages

are as follows; Kikai-Akahoya volcanic ash (K-Ah: 7,300 cal BP), Sakurajima-

Satsuma volcanic ash (Sz-S: 12,800 cal BP) Aira-tanzawa volcanic ash (AT:

30,000 cal BP), and Osumi fall pumice (A-Os: 30,000 cal BP). Both AT and A-

Os are erupted from the Aira caldera at the same time.

Figure 3. Microphotographs of the main phytolith morphotypes observed in this study.

a: *Sasa*-type (BULLIFORM FLABELLATE)　b:*Pleioblastus*-type (BULLIFORM FLABELLATE)　c: Bambusoideae-type (BULLIFORM FLABELLATE) d: Andropogoneae-type (BULLIFORM FLABELLATE) e: Panicoideae-type (BLOCKY) f: Bambusoid-type (SADDLE) g: Chloridoid-type (SADDLE) h: BILOBATE i: RONDEL j: POLYLOBATE k: CROSS l: CRENATE m: ACUTE BULBOSUS n: ELONGATE o: *Castanopsis*-type (POLYHEDRAL FACETATE) p: *Litsea*-type (ELONGATE GENICULATE SINUATE) q: *Distylium*-type (ELONGATE BRACHIATE ENTIRE) r: Jigsaw-puzzle type (IRREGULAR SINUATE)

Scale bar is 20 μm.

Figure 4. Percentage occurrences of phytolith morphotypes at Site 1 and Site 2

Figure 5. Percentage occurrences of phytolith morphotypes at Site 3

Figure 6. Vegetation transition in the southernmost part of Kyushu District inferred from phytolith and pollen records, with representative phytolith and pollen types and

the LR04 marine isotope stack (Lisiecki and Raymo, 2005) between the terminal Pleistocene and the early Holocene. The pollen records were reported by Matsushita (2002), Iwauchi and Hase (1996), Hase and Hatanaka (1984), and Iwauchi and Hase (1995).

Table 1. Radiocarbon ages of humin fractions extracted from the paleosols at Site 3. [14]C dates were calibrated to calendar years using the program Calib Rev 8.1 and the IntCal20 calibration dataset (Reimer et al., 2020).

Table 2. Summary of plant families and genera producing phytolith types identified in this study and their habitat and climate zones. The phytolith type produced from the respective plant families, subfamilies, tribes, and genera are based on the following references; [*1] Sugiyama and Fujiwara (1986), [*2] Kondo and Ohtaki (1992), [*3] Kondo and Sase (1986), [*4] Sugiyama et al. (1988), [*5] Kawano et al. (2012), [*6] Sase and Kondo (1974), and [*7] Kawano (2008).

Supplementary data

Supplementary Figure 1. Age model of the layers at Site 3. The black dots and bars

indicate the calibrated radiocarbon ages and the ages of volcanic ashes, respectively.

Supplementary Table 1. (a) Raw data for number of each phytolith type observed in this study and phytolith concentrations and (b) Percentage occurrence in each phytolith type calculated from the observed number of the phytolith

(A)
140°E
130° E
40° N
Japan
Kyushu District

(B)
130°E   1,2■   131°E
1■   *Aira caldera*
3■   *Sakurajima volcano*
Satsuma Peninsula   4■   *Osumi Peninsula*
31°N
Kikai caldera
30 km
■ Previous palynological study site

(C)
130°30' E   131°00' E   31°20' N
Site 3
Site 1   Site 2
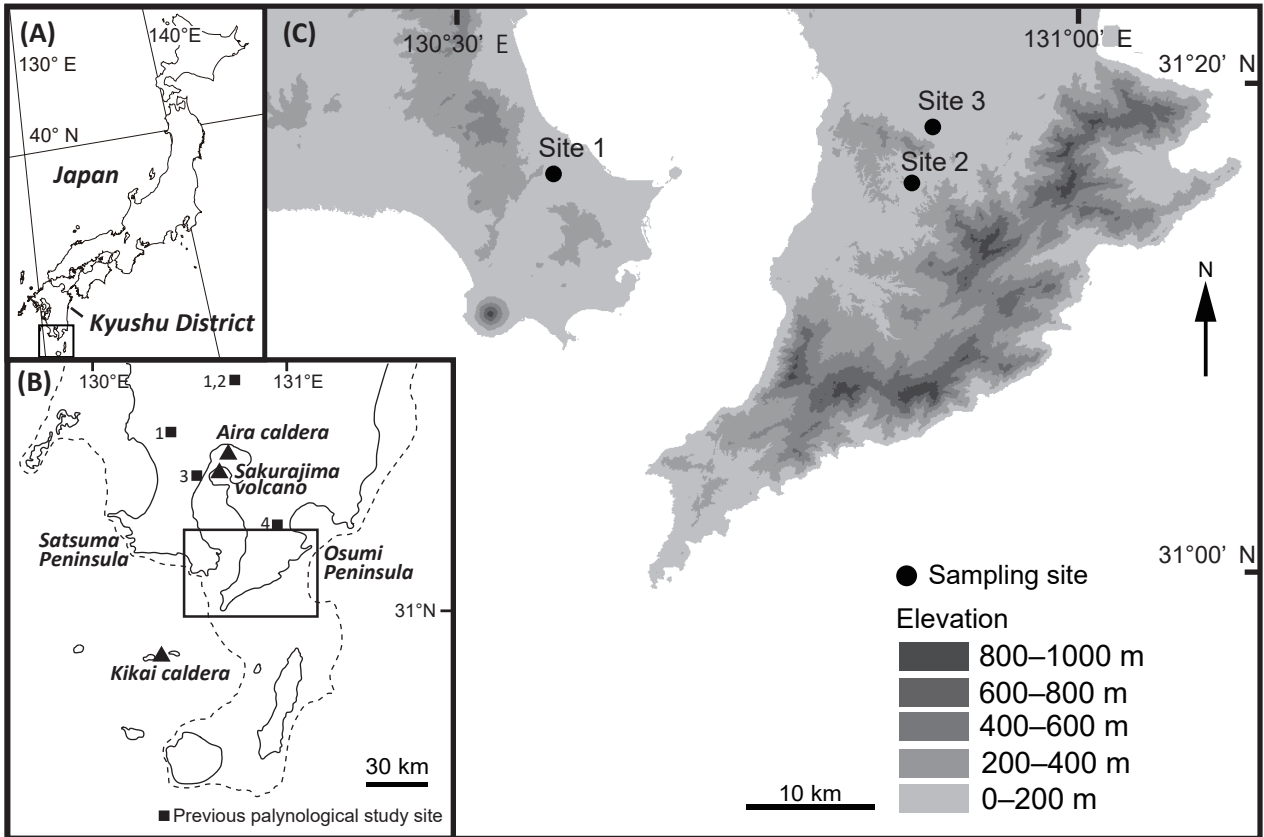N
● Sampling site
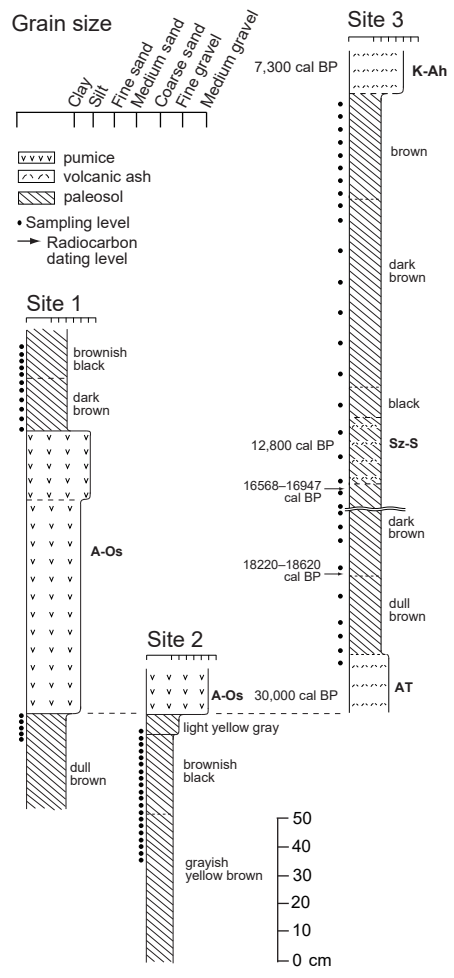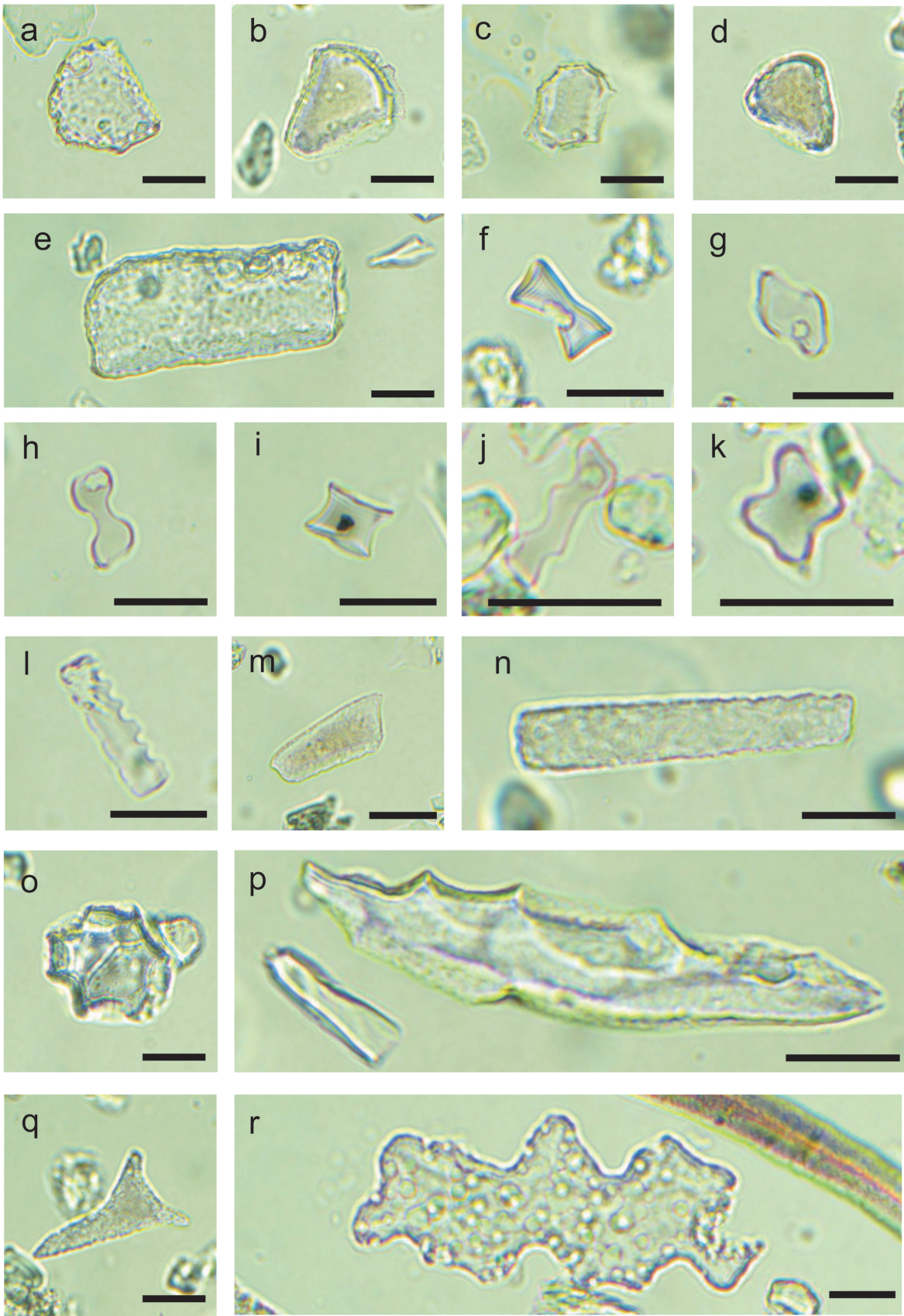Elevation
800–1000 m
600–800 m   31°00' N
400–600 m
200–400 m
10 km   0–200 m

Figure 1

Figure 2

Figure 3
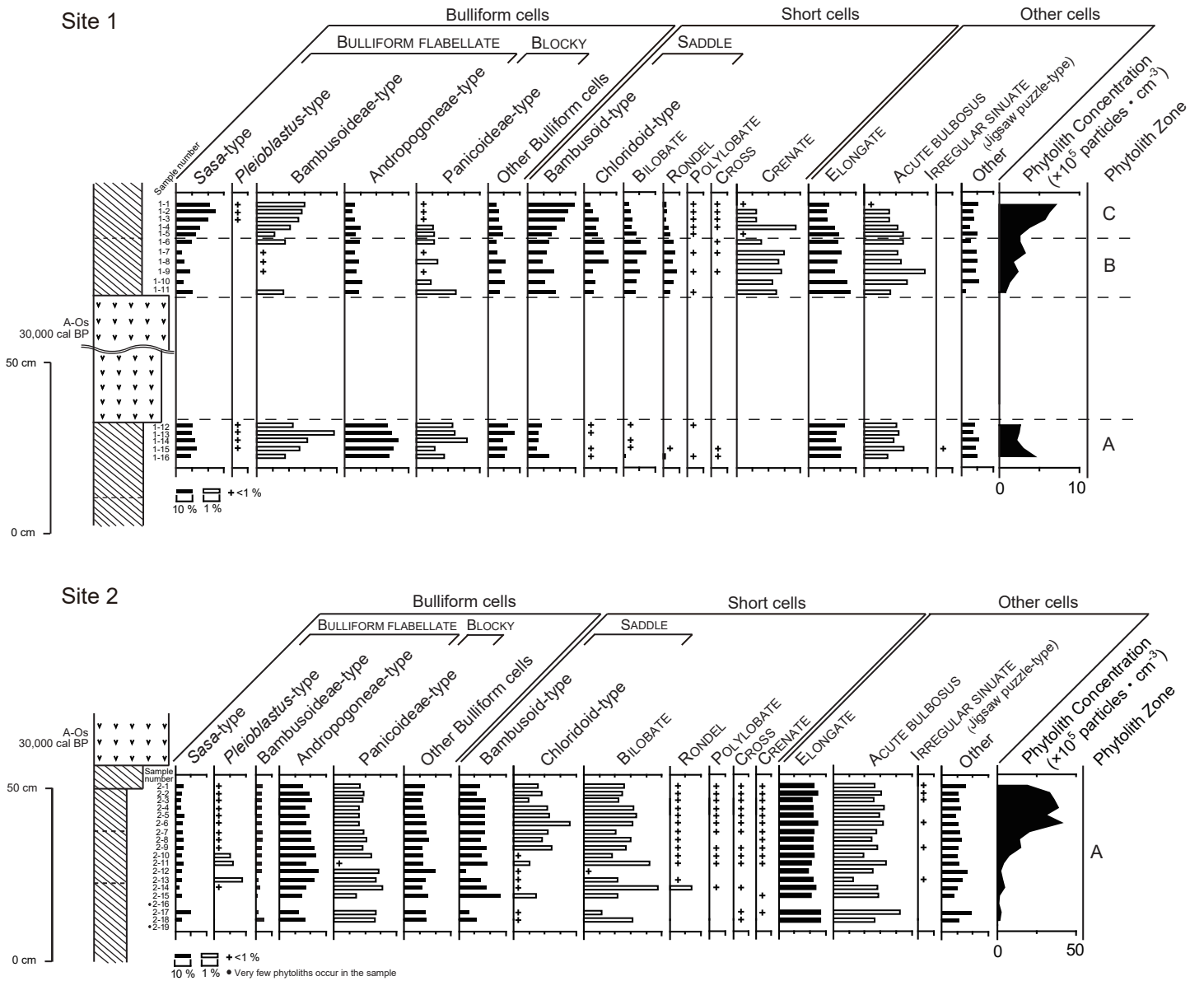
Figure 4
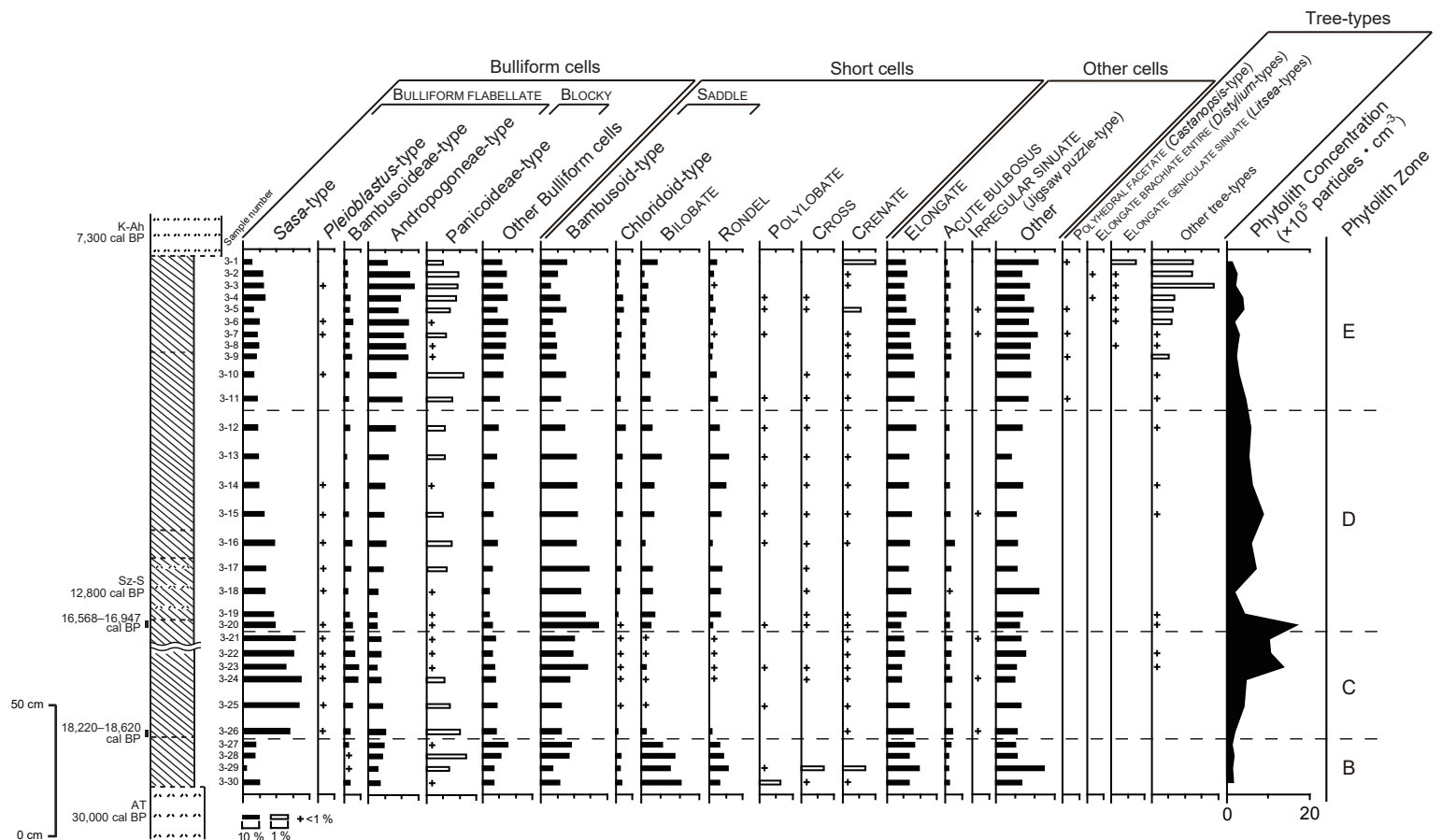
Figure 5
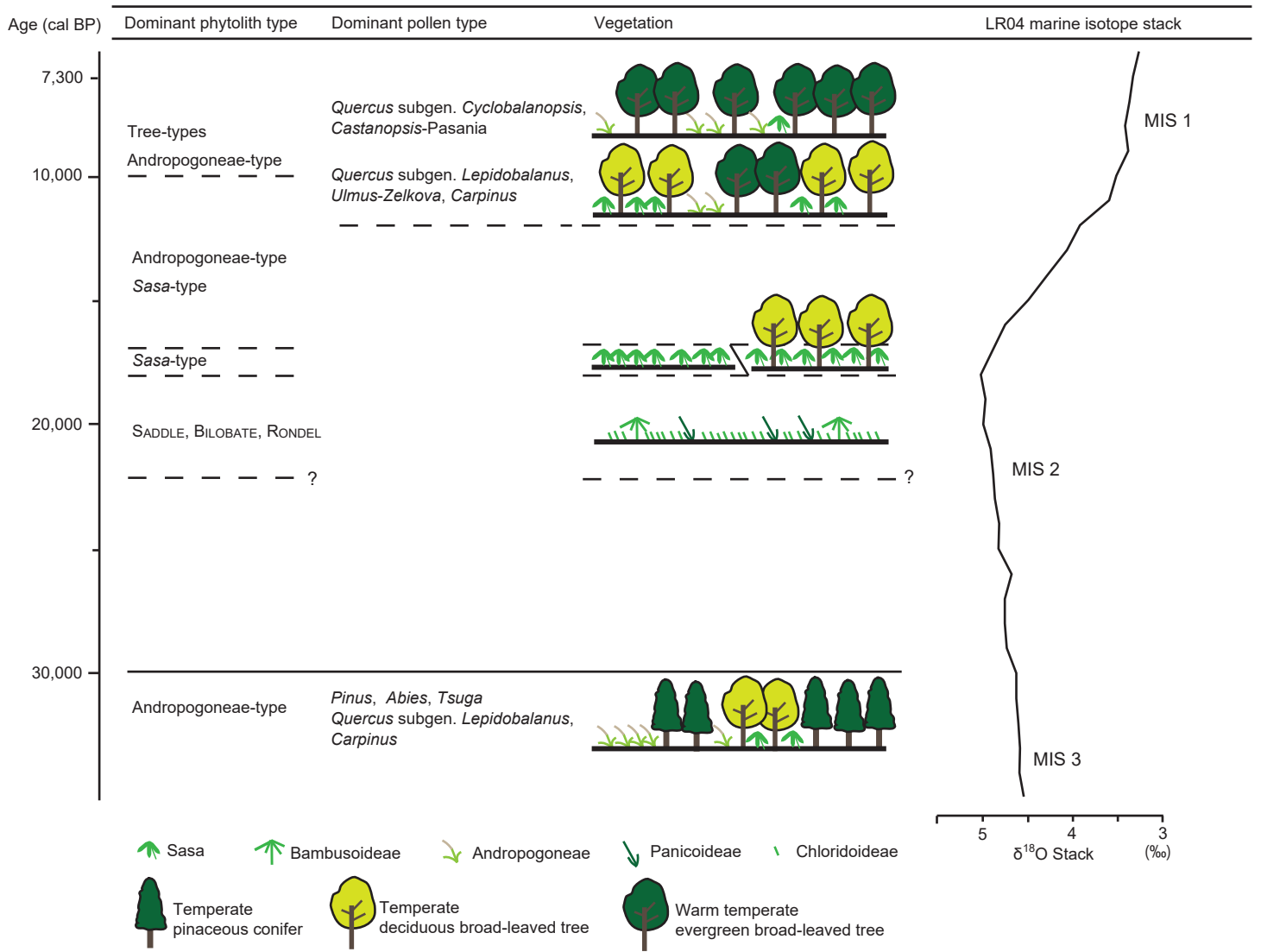
Figure 6

Table 1

Sample site	Sampe number	^{14}C date BP ±1σ	Cal BP with 2σ error	δ^{13}C(‰)	Material	Code
3	3-20	13800 ± 40	16568–16947	−20.53	Humin fractions	Beta- 597151
3	3-26	15040 ± 40	18220–18620	−20.91	Humin fractions	Beta- 597150

Table 2

Family, Subfamily, or Tribe	Genus	Carbon fixation type	Main habitat	Climate zone	Produced phytolith-type
Herbs					
Bambusoideae					Bambusoideae-type (B$_{ULLIFORM FLABELLATE}$)[1], Bambusoid-type (S$_{ADDLE}$)[2]
	Sasa	C$_3$	Grassland Understory of decidious forest	Subarctic–Cool-temperate zone	*Sasa*- type (B$_{ULLIFORM FLABELLATE}$)[1,3]
	Pleioblastus	C$_3$	Grassland	Warm-temperate zone	*Pleioblastus*- type (B$_{ULLIFORM FLABELLATE}$)[1,3]
Panicoideae					Panicoideae-type (B$_{ULLIFORM FLABELLATE}$)[4,5] B$_{ILOBATE}$, P$_{OLYLOBATE}$, R$_{ONDEL}$, C$_{ROSS}$
Andropogoneae (*Miscanthus*)		C$_4$	Grassland, Bare land	Cool-temperate–Warm-temperate zone	Andropogoneae-type (B$_{ULLIFORM FLABELLATE}$)[5,6]
Chloridoideae		C$_3$ & C$_4$	Grassland (especially pasture) Bare land	Cool-temperate–Warm-temperate zone	Chloridoid-type (S$_{ADDLE}$)[2], R$_{ONDEL}$
Pooideae		C$_3$	Grassland (especially pasture)	Subarctic–Cool-temperate zone	C$_{RENATE}$
Trees					
Deciduous broad-leaved tree					Jigsaw puzzle-type (I$_{RREGULAR SINUATE}$)[7,8]
Quercoideae					
	Castanopsis	C$_3$	Forest	Warm-temperate–Subtropical zone	*Castanopsis* -type[7] (P$_{OLYHEDRAL FACETATE}$)
Hamameloideae					
	Distylium	C$_3$	Forest	Warm-temperate–Subtropical zone	*Distylium* -type[7] (E$_{LONGATE GENICULATE SINUATE}$)
Lauraceae					
	Litsea	C$_3$	Forest	Warm-temperate–Subtropical zone	*Litsea* -type [7] (E$_{LONGATE BRACHIATE ENTIRE}$)
Ferns					
Dennstaedtiaceae					
	Pteridium	C$_3$	Glassland	Cool-temperate–Subtropical zone	Jigsaw puzzle-type (I$_{RREGULAR SINUATE}$)[7,8]